Dynamics of diluted antiferromagnetic Ising spin systems on the fcc lattice

Marta Z. Cieplak*
Department of Physics and Astronomy, The Johns Hopkins University, Baltimore, Maryland 21218

Tomasz R. Gawron†
Department of Theoretical Physics, University of Lund, S-22362 Lund, Sweden

Marek Cieplak†
Department of Physics and Astronomy, The Johns Hopkins University, Baltimore, Maryland 21218
(Received 13 September 1988; revised manuscript received 4 November 1988)

We consider Glauber dynamics of Ising spins randomly populating sites of the fcc lattice and coupled by nearest-neighbor antiferromagnetic interaction J. This investigation extends our former studies of small clusters beyond the percolation threshold and is aimed at modeling semimagnetic semiconductors. The energy barriers against inversion of local energy minima are found to be integer multiples of $2|J|$. If small next-neighbor interactions, J_{NN}, are taken into account, the distribution of the barriers remains peaked at these values. The spectrum of relaxation times may then contain gaps at low temperatures, depending on relative strength of J_{NN} to J. We have studied dynamics of the system for $J_{NN}=0$ in Monte Carlo simulations. Decays of time delayed single- and two-spin correlations, above the critical temperature, are found to be consistent with that given by a sum of distinct exponential terms. We also studied the dynamic spin susceptibility by applying an oscillatory magnetic field and by monitoring oscillations in the induced magnetization for small frequencies ω. The susceptibility is found to show structure as a function of $\log\omega$.

I. INTRODUCTION

The fcc antiferromagnetic system of N Ising spins coupled by nearest-neighbor forces is known to be fully frustrated.[1-3] The ground state has an energy of $-2N|J|$ and its degeneracy is of order $e^{N^{1/3}}$.[2] The first four excited states have energies 8, 12, 16, and 20 in units of $|J|$. For classical Heisenberg spins the ground state has energy also equal to $-2N|J|$ and it still possesses a large nontrivial degeneracy.[4,5] For both systems the degeneracy can be significantly reduced by next-nearest-neighbor couplings and anisotropies. Thermal fluctuations and quenched disorder due to spin removal also brake degeneracies.[5] Dilution may even favor noncolinear arrangements of the Heisenberg spins.[6] Diluting the Ising system below the occupational probability, x, of 50% or so leads to a spin-glass (SG) behavior studied in several numerical simulations.[7] In the case of isotropic Heisenberg spins no equilibrium SG phase is expected to exist.[8,9]

The diluted antiferromagnetic spin systems with short-range couplings are good models of the so-called semimagnetic semiconductors[10] like $Cd_{1-x}Mn_xTe$ and $Hg_{1-x}Mn_xTe$ and systems like MnO_{1+x} (Ref. 11) which are apparently SG's in a range of values of x. The spins in these systems have certainly (quantum) Heisenberg nature but additional anisotropic terms turn the equilibrium properties to Ising-like. The anisotropy could be due to the Dzyaloshinski-Moriya coupling[12] which is known to make Ruderman-Kittel-Kasuya-Yosida Heisenberg SG undergo a phase transition with the Ising critical exponents.[13]

The semimagnetic semiconductors are possibly "cleanest" SG's to study since their properties in most cases can be explained in terms of a single-exchange coupling the value of which is well known. In the case of $Cd_{1-x}Mn_xTe$ $J=-13.8\pm0.3$, as obtained from susceptibility measurements,[14] or -13.4 ± 0.2 as obtained from neutron scattering experiments.[15] The next-nearest-neighbor coupling is antiferromagnetic and is of order 0.1–0.2 of that value.[16]

The static magnetic properties of the "semimagnetic" SG's appear to be similar to that of metallic SG's. This is not surprising for the following reason. The Ising spins on the fcc lattice experience local exchange fields similar to those felt by Ising spins on an fcc lattice but coupled by $+J$ or $-J$ exchange constants, each with probability of $\frac{1}{2}$. In three dimensions an effective block coupling energy of this bimodal SG grows with the size of the system and the corresponding exponent is equal to that found for the Gaussian probability of the couplings.[9] Since the effective coupling grows to infinity, the discretization in units of the microscopic exchange coupling ceases to be noticeable and thus the bimodal SG should be no different from the Gaussian one.

Can dynamic properties of magnetic semiconductors be different than those characteristic of the metallic ones? In this paper we shall argue that they could, provided the effective Ising nature of the spins also prevails in the gross dynamical behavior. It should be noted that the Glauber dynamics of Ising spins is purely relaxational whereas the Heisenberg systems allow also for spin waves.[17] Spin waves should not matter at long times relevant for SG's but this point requires an investigation. On the other hand, the six-state nature of Mn ions or

longer-ranged couplings may smooth out sharp features in relaxation of the two-state Ising model. It still seems that a good starting point to study dynamics is to find out what are the predictions of the Ising model and then to confront them with experiment to judge about the Heisenberg effects, if any.

Studying Ising spin dynamics on the fcc lattice has actually been our task in a previous paper,[18] which dealt with the situation found below the (nearest-neighbor) percolation threshold, $x_c = 0.195$. For such small concentrations, the system consists of finite clusters, the Glauber dynamics of which could be solved exactly. The major finding was that, for the dynamics, the discrete nature of the exchange coupling does play a role since it discretizes energy barriers and therefore it discretizes possible time scales of relaxation. For Gaussian SG's the energy barriers take continuum of values and the relaxation ties form a smooth spectrum.[19] On the other hand, in our case the spectrum should develop gaps at sufficiently low temperatures: The relaxation times are expected to relate to the barriers via the Arrhenius law. In our former paper we have studied clusters made of up to seven spins. These allowed for three values of barriers: 0, $2|J|$, and $4|J|$, and thus for a three-peaked distribution of the relaxation times on a logarithmic scale. This in turn resulted in a structured dynamic susceptibility. Its real part χ' had three plateaus, and its imaginary part three maxima when plotted against $\log\omega$. The maxima are located at inflection points of χ'. The temperature dependence of the dynamic susceptibility was rather standard and similar to that found, e.g., by Gunnarsson[20] in a short-ranged SG in which ferromagnetic and antiferromagnetic bonds are mixed (except that the freezing temperature in clusters vanishes).

In this paper we extend our analysis to systems above the percolation threshold. In Sec. II we study structure of the density of local energy minima, and in Sec. III we discuss distribution of barriers required to invert typical energy minima. In Sec. IV we study time decay of spin correlations by means of a Monte Carlo simulation and finally, in Sec. V, we analyze dynamic susceptibility. The susceptibility is calculated in a simulation in which a small oscillatory magnetic field is added to the Hamiltonian and the oscillations in the induced magnetization are monitored. Our method limits the studies to small time periods but is does point to a structured dynamical susceptibility above the threshold.

II. LOCAL ENERGY MINIMA

The Hamiltonian of the system under consideration is given by

$$H = -\sum_{i,j} J_{ij} S_i S_j \ , \tag{1}$$

where $S_i = \pm 1$, and i counts only occupied sites. The exchange couplings are equal to $J < 0$ when the sites form a pair of nearest neighbors and are zero otherwise. The fcc lattice can be thought of as composed of four $L \times L \times L$ interpenetrating simple cubic sublattices. The number of spins it contains is on average equal to $N = 4L^3$. The periodic boundary conditions are adopted.

In order to obtain the largest barrier, giving rise to the longest relaxation time one should first find the ground state. This barrier is equal to energy required to invert the spin configuration in this state upside down.[21,22] The only way to find a ground state (for $x_c < x < 1$) for the fcc lattice appears to be performing extensive Monte Carlo quenches as in the paper by McMillan.[23] However, reliable results even for a $4 \times 4 \times 4$ bimodal SG require of order 2^{16} quenches per sample.[24]

Clearly, studying the fcc systems would require taking N larger than 64, but this is prohibitive computationally. Instead we select random local energy minima as obtained by a gradual decrease of temperature to zero. Typically, we run the system at $T = 2$ (in units of $|J|/k_B$) and quench the successive configurations by applying temperature decrements of 0.5 and performing at least ten Monte Carlo steps per spin at each $T < 2$. For each concentration x studied, we took into account typically 100 samples and identified 100 local energy minima in each of them. We then calculated energy barriers against inversion of these minima. These barriers are hoped to be responsible for "typical", but not the longest, relaxation times. Our purpose here is qualitative: to demonstrate a large range of discrete values that energy barriers may take in the system.

Figure 1 shows histogram of energies per spin of the lo-

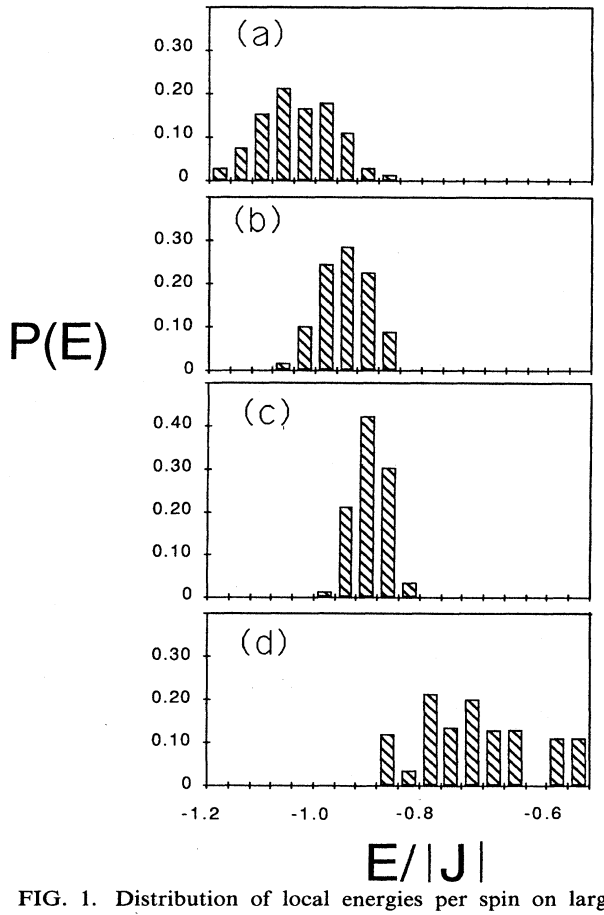

FIG. 1. Distribution of local energies per spin on largest clusters. Figures (a) through (d) correspond to concentrations $x = 0.30$, 0.22, 0.18, and 0.08, respectively. At the highest two concentrations the systems are above the percolation threshold.

cal energy minima obtained by our quenching procedure. For each sample of a given x the largest cluster was selected. Above the percolation threshold ($x=0.3$ and 0.22) such clusters are percolating and below ($x=0.18$ and 0.08) they do not span the system. The local energy minima shown in Fig. 1 are the minima obtained for the largest clusters and with $L=5$. Clearly, the larger the connectivity the smaller the average energy. For $x=1.0$ (not shown in the figure) energies of the minima group in the vicinity of -2, i.e., the exact ground-state energy per spin. Slower quenching rates generally shift the distributions towards lower energies. One expects the low-energy tail to give rise to the larger barriers, and this indeed is the case. A total energy of the system contains also contributions from all of the smaller sized, i.e., nonpercolating, clusters (including those consisting of single spins). These enhance the high-energy tail of the distribution considerably (not shown in the figure) and the corresponding barriers are small.

III. ENERGY BARRIERS

Our algorithm of search for the barriers is related to the "landscape exploration" method of Rammal and Benoit[25] and is almost the same as used by Banavar, Cieplak, and Gawron[26] in studies of the Gaussian and bimodal SG's. There are two differences here though: (1) we deal with randomly selected local energy minima and not with the ground states, and (2) we restrict our searches to phase-space trajectories in which each spin is inverted once. An outline of the algorithm is as follows.

Each reversal trajectory is characterized by an energy $\Delta E_{\max}$, in excess of the local-energy minimum, corresponding to the highest point on the trajectory. A barrier, B, is defined as the smallest $\Delta E_{\max}$. We select a first tentative value, B_1, of barrier against reversal of the whole system and a resolution, R, within which B will be determined. Here we take $R=0.1$. We check whether one can find trajectories of spin reversals that do not require a supply of more than B_1 of energy. If no allowed trajectory is found, we conclude that B_1 is too small an estimate of B and we update B_1 to

$$B_2=B_1+R \ . \tag{2}$$

If at least one allowed trajectory is found we take note of $\Delta E_{\max}$ of the last such trajectory considered and update B_1 to

$$B_2=\Delta E_{\max}-R \ . \tag{3}$$

We repeat the search with B_1 replaced by B_2. We continue in this way until after one successful choice of B_ν we get to $B(\nu+1)$ which fails to produce an allowed inversion. The barrier B is then given by B_ν within the resolution R.

Consider first the largest (i.e., percolating above x_c) clusters in the systems. Figure 2 shows distributions of the barriers obtained for the local-energy minima in the largest clusters as generated for $L=5$ and for several values of x.

The smallest concentration of $x=0.08$ corresponds to

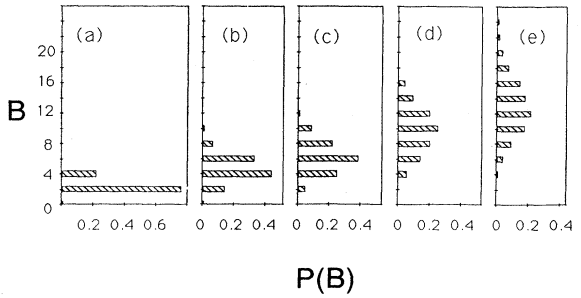

FIG. 2. Distribution of energy barriers for largest clusters generated at five values of x. The system size is $L=5$. The barriers here are defined as smallest energies required to invert local energy minima. (a)–(e) Concentrations 0.08, 0.18, 0.22, 0.30, and 0.35, respectively.

the regime considered by us in Ref. 18. As before we find here only barriers of values 0, $2|J|$, and $4|J|$. An individual cluster may contain minima with one, two, or all of these barriers. A connection between a barrier, B, and corresponding relaxation time goes via the Arrhenius law

$$\tau_\nu=a\tau_0 e^{B/k_BT} \ , \tag{4}$$

where τ_0 is the microscopic Glauber time,[27] usually assumed to be of order 10^{-12} s. The factor a reflects an actual geometry of the cluster and is of order unity.[28] A collection of clusters contributing to a given B yields a collection of different a's. This leads to some T-dependent spread around selected values of the allowed relaxation times, as discussed in Ref. 18. At sufficiently low T, time scales corresponding to various B's separate out and the relaxational spectrum develops gaps.

Increasing x to higher values produces a gradual increase in occurrence of larger barriers. They always come in multiples of $2|J|$. For $x=0.18$ we have found barriers up to $10|J|$. At this x there is no percolation yet. The value of $10|J|$ derives from small clusters. Above the percolation threshold still larger barriers are expected to appear and indeed they do as shown in Fig. 2. At $x=0.35$, we get barriers between 0 and $24|J|$. It should be noted that percolating clusters may have local energy minima which require little energy to overturn. These give rise to faster processes.

Above x_c, the system consists of the percolating cluster and of many small clusters. All these clusters can be overturned individually. Thus a distribution of barriers required to invert the whole system looks very much like in Fig. 2 except for an increased weight at small B's, mainly at $B=0$ and $2|J|$. For the purpose of the discussion of our Monte Carlo results in the next two sections, note that at $x=0.22$, i.e., just above x_c, the percolating cluster has a sizable portion of minima with small barriers.

The distribution of the barriers, $P(B)$, depends on the class of the local energy minima one gets during quenching. We have compared $P(B)$ obtained by two different quenching schemes. Both schemes start from a Monte Carlo trajectory at $T=2$. In one scheme a gradual decrease in T occurs in 50 Monte Carlo steps per spin and

in the other one in 2500 such steps. For a system with $L=5$ and $x=0.22$ fast colling yields an average B, $\langle B \rangle$, of $6.2|J|$. The slower cooling, on the other hand, gives $\langle B \rangle$ of $7.5|J|$, extending $P(B)$ towards larger values of B. Overall features, however, remain the same.

It is interesting to find out, what is the size dependence of the average barriers obtained. Fisher and Huse[29] postulate that largest B's should grow as a power law of the linear size of the system. The exponent of this power law should not exceed $D-1$, where D is the spatial dimensionality. In $D=2$ models, with single spin-flip phase-space trajectories we get the limiting linear-law dependence.[19] In the case of the fcc model, however, the lack of availability of the true ground states makes meaningful studies of the L dependence impossible: $\langle B \rangle$ depends on the cooling rate. All we can see is that $\langle B \rangle$ grows with L. For instance for $x=0.22$ and the faster cooling rate we get $\langle B \rangle$ of 3.9, 5.0, 5.7, and 6.6 for $L=3$, 4, 5, and 6, respectively. This suggests a linear growth, but we believe this to be an artifact of selecting minima which are not sufficiently close to the true ground state to produce low-T scaling laws.

We can determine, however, that $\langle B \rangle$ depends mainly on the connectivity. If we take ensembles of percolating clusters at two concentrations and adjust values of L so that on average the two ensembles have similar numbers of spins, then the bigger x, the bigger $\langle B \rangle$. For instance for $x=0.22$ and $L=6$ percolating clusters have on average 136 spins and a mean barrier of 6.6 (with the faster cooling rate). For $x=0.40$ and $L=4$, such clusters contain on average 101 spins but $\langle B \rangle = 10.1$.

Despite the qualitative nature of our studies of the barriers, it is clear that both largest clusters and whole systems have states in which the barriers range from $2|J|$ to many multiples of $2|J|$. The bigger x and the bigger L, then the more weight is carried by the large barriers. In the vicinity of x_c though, the smaller barriers do have substantial weight. The discreteness of barriers leads to a geometrical sequence of the relevant time scales. Take, for instance, $T=0.3$ and use Eq. (4). Then for $B=2$, 4, 6, 8, 10, and $12|J|$ the relaxation times, in seconds, are of order of the following powers of 10: -9, -6, -4, -1, 2, and 5, which makes a considerable range. The separation of various time scales decreases significantly with T; e.g., for twice as high T, B of $12|J|$ gives τ of order 10^{-4} s and is about 20 times longer than τ corresponding to $B=10|J|$. At still higher T the differences between the various time scales become less and less significant. The question we shall ponder now is whether the discrete structure of time scales predicted for low T's can be seen in quantities one measures.

IV. TIME-DELAYED SPIN CORRELATIONS

One common way to characterize dynamical behavior of a magnetic system is to specify the single-spin time-delayed correlation function. This function is defined as

$$G(t)=\frac{1}{N}\sum_{i=1}^{N}\langle S_i(0)S_i(t)\rangle \ , \tag{5}$$

where the angular brackets denote the thermal average. We calculate $G(t)$ by the Monte Carlo method. We first check its effectiveness by determining $G(T)$ for the six-spin cluster in which an open chain of four spins attaches one spin to the second site and one spin to the third site. This is one of the 137 clusters studied exactly in Ref. (18). This cluster has $B=4|J|$. For each T we started from random initial configuration and averaged the data over 1000 different time trajectories (i.e., different strings of random numbers). $G(t)$ was then plotted versus t as measured in Monte Carlo steps per spin. Except for some transient effects at short times, the decay was given by a single exponential law

$$G(t)=G_0\exp(-t/\tau) \ . \tag{6}$$

The relaxation time was found for six temperatures and its T dependence is well described by the Arrhenius law, Eq. (4), where $B=4|J|$ and $a=0.29$, which agrees with Ref. (18). This sets our confidence in the method.

We chose the following systems for a detailed analysis: (a) $L=14$, $x=0.08$, consisting of 878 spins (b) $L=12$, $x=0.12$, with 829 spins, and (c) $L=10$, $x=0.22$, consisting of 880 spins (out of which 580 are in the percolating cluster). We do not perform any averages over samples here.

The idea here is to study systems containing similar numbers of spins and, in the case of system (c), to discuss the situation very close to the threshold, where the small barriers are more abundant than for larger x. The corresponding time scales become then accessible in the simulation. System a is chosen to make direct comparisons with Ref. 18. In each case the sample was cooled to $T=0.5|J|/k_B$ and the correlations were studied at this T. This choice is a compromise between a desire to take T sufficiently low to separate the time scales and a necessity to take it high enough to avoid numerical inaccuracies and to make the calculations reasonably fast. In Ref. 18 we were able to study $T=0.2$ and $0.3|J|/k_B$. We expect that in the case of system c the temperature of $0.5|J|/k_B$ is above the critical temperature for the SG paramagnet transition because this system is just above the percolation threshold.

In order to allow for proper equilibration, we skip the first 5000 Monte Carlo steps per spin (MCS/S) before we start monitoring $G(t)$. The correlation function was then calculated through 4000 MCS/S in the case of systems a and b and 10 000 MCS/S in the case of system c. In each case $G(t)$ is averaged over about 400 starting configurations. These were selected to be the last spin configurations obtained in a previous run.

We expect to identify at least four following distinct time scales: (a) of order of a few MCS/S and related to $B=0$, (b) of order 5–30 MCS/S coming from states with $B=2|J|$, (c) of order 300–1500 MCS/S corresponding to $B=4|J|$, (d) of order 2500–10 000 MCS/S corresponding to $B=6|J|$. In Ref. 18 the up to seven-spin clusters we considered did not have any barriers equal to $6|J|$. At $x=0.08$ larger clusters, however, are present and they contribute to the larger barriers. The numbers of MCS/S listed previously were chosen in fact *a posteriori,* in the interpretation process, and they reflect selfconsistency of various data presented herein. They also reflect the fact

that effective average a factors associated with groups of relaxation times having same barriers tend to be smaller than 1 (e.g., in the six-spin cluster discussed before, $a=0.29$).

Figure 3 shows $G(t)$ for the two systems in which $x<x_c$. The decomposition of the decay into separate exponentials is a bit arbitrary, particularly at this moderate T. Nevertheless by plotting $\ln G(t)$ versus t we can identify three different slopes (which are measures of $1/\tau$) corresponding to the three regimes B, C, and D as indicated by the straight lines. It should be noted that systems a and b behave similarly.

The existence of separate exponentials in the decays of $G(T)$ above the threshold is less compelling but, as shown in Fig. 4, we can easily identify region D, corresponding to the barriers equal to $6|J|$. In the same figure we compare $G(t)$ as obtained by considering spins which belong to the percolating cluster to that obtained for the whole system. It is clear that the two decays are quite similar and thus the contribution of the percolating cluster is dominating.

Figure 4 is shown in the scale of 10 000 MCS/S. If we concentrate on the initial time behavior, demonstrated in Fig. 5, then we can also identify regions A and B. We failed, however, to locate region C above the percolation threshold uniquely. This may be due to a possible overlap of B with C at this T. Figure 5 compares relaxation times of the region B in the three systems studied. In region B these times are all of the same order. They depend on x due to variations in the a factors.

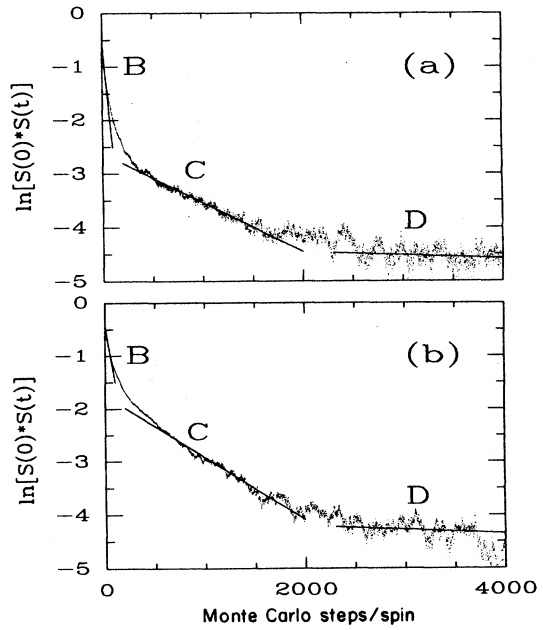

FIG. 3. Time dependence of $\ln G(t)$ $x<x_c$. Straight sections correspond to decays dominated by a single exponential. (a) $x=0.08$ and (b) $x=0.12$. Region A cannot be shown in this scale of the figure. In the case of system (a) $\ln\tau/\tau_0$ is effectively 4.0, 6.99, and 9.64 for regions B, C, and D, respectively. In the case of system (b) these numbers are correspondingly 4.4, 6.75, and 9.55.

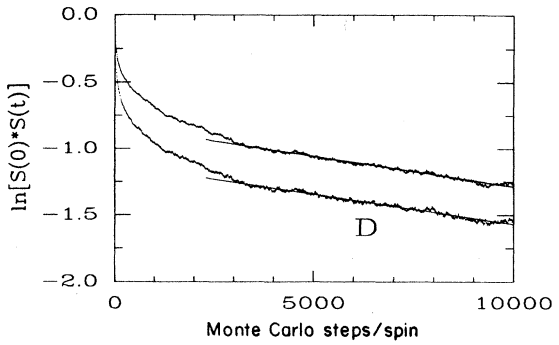

FIG. 4. Time dependence of $\ln G(t)$ just above the percolation threshold, $x=0.22$. The top line refers to the percolating cluster and the bottom line to decays averaged over all spins in the system. In both cases the effective relaxation times in the region D have logarithms close to 10.0.

So far we were concerned with decays of the single-spin correlations, related to the dynamic susceptibility. As pointed out in Ref. 30, decays of two-spin correlations relate to the energy fluctuations and hence to the dynamic specific heat. In the absence of a static magnetic field the relaxation spectrum of the two-spin correlations is expected to be similar to that of the single-spin ones expect for the lack of the very longest time.[30] As a measure of the two-spin correlations we took

$$H(t)=\frac{1}{N}\sum_{i=1}^{N}\left[\frac{1}{n}\sum_{j=1}^{n}S_i(0)S_i(t)S_j(0)S_j(t)\right]. \tag{7}$$

In this definition, n denotes the local number of coupled nearest neighbors ($n\leq 12$). The function $H(t)$ tends to a constant value, H_0, which needs first to be approximately determined. To this end we took the last 1000 time steps (out of 10 000) in the case of $x=0.22$, or 100 steps (out of 4000) for $x=0.08$, to average out and get H_0. We subtract H_0 from $H(t)$ and get a function which now decays

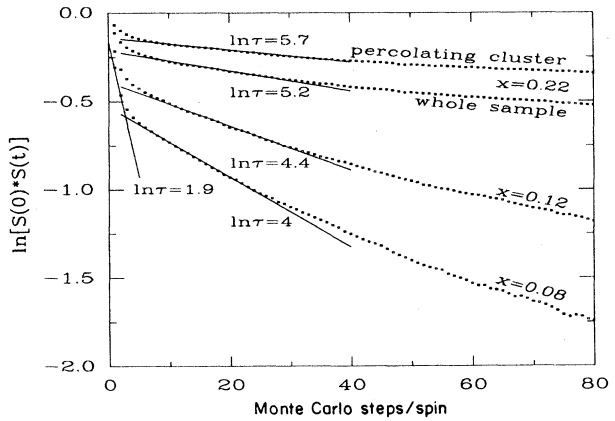

FIG. 5. Time dependence of $\ln G(t)$ for all the three systems studied, shown in the region of small time scales. The line representing the steeper slope indicates region A. All other slopes mark off region B. The corresponding effective relaxation times are shown, in units of τ_0.

to zero. We have found that these correlations decay much more rapidly and region D is already in the noise level. Nevertheless, the relaxation times corresponding to regions B and C are consistent with those found for the single-spin correlations. This supports the idea of similarity of the single- and two-spin spectra also in our system.

V. DYNAMICAL MAGNETIC SUSCEPTIBILITY

The time-dependent correlations discussed in the previous section are quantities that can be determined in an equilibrium. Another way of characterizing the dynamics is to perturb the system by ac magnetic field and to monitor oscillations in the induced magnetization, $m(t)$. In this experiment the system is displaced slightly away from equilibrium. In order to determine the resulting dynamic susceptibility one should switch on a small amplitude field,

$$h = h_0 \sin(\omega t) , \tag{8}$$

at $t=0$ and then start monitoring the magnetization after some time t_0, chosen so that all transient exponentials can be considered extinct.

Getting beyond t_0 in a Monte Carlo simulation is often impossible and as far as we know nobody has attempted to determine a dynamical susceptibility in this way. Our purpose, however, is rather modest: We want to find out whether the discrete nature of the relaxation spectrum is capable of building a frequency-dependent structure. We then adopt the following approximate procedure. First of all, we choose $T=0.5$ and focus on the high-frequency, i.e, short-time, domain. We choose t_0 to be 50 000 MCS/S so that the responses in regions A through D should be fairly well defined. We select a range of periods of oscillations, $T_0=2\pi/\omega$, between 10 and 40 000 MCS/S. In this way, region A is ruled out: too rapid variations in the field make it hard to maintain the system close to equilibrium. We take h_0 to be equal to $0.1|J|$.

Once we pass the point $t=t_0$, we average $m(t)$ over many periods and extract the real and imaginary parts of the susceptibility through

$$m(t)=h_0[\chi'\sin(\omega t)-\chi''\cos(\omega t)] . \tag{9}$$

For periods T_0 less than 200 MCS/S we monitor $m(t)$ for 10 000 MCS/S which yields between 50 and 1000 periods, depending on T_0. For T_0 between 200 and 3000, we needed about 150 periods. For still larger periods (up to 40 000), we had to limit our averages to 30 periods. The error bars then increase with T_0. Certainly, the longer-lived transients still keep decaying throughout the full Monte Carlo evolution, but this appears to make no more than a small perturbation to the susceptibility in the frequency domain considered.

The results of our calculations are presented in Fig. 6. Consider first the system at $x=0.08$. It is seen that the plots of χ' and χ'' versus $\log_{10}(\omega)$ show the same structure as predicted in Ref. 18 by more precise means: χ'' displays a sequence of maxima where χ' crosses over from one plateau to another. These occur, roughly, at

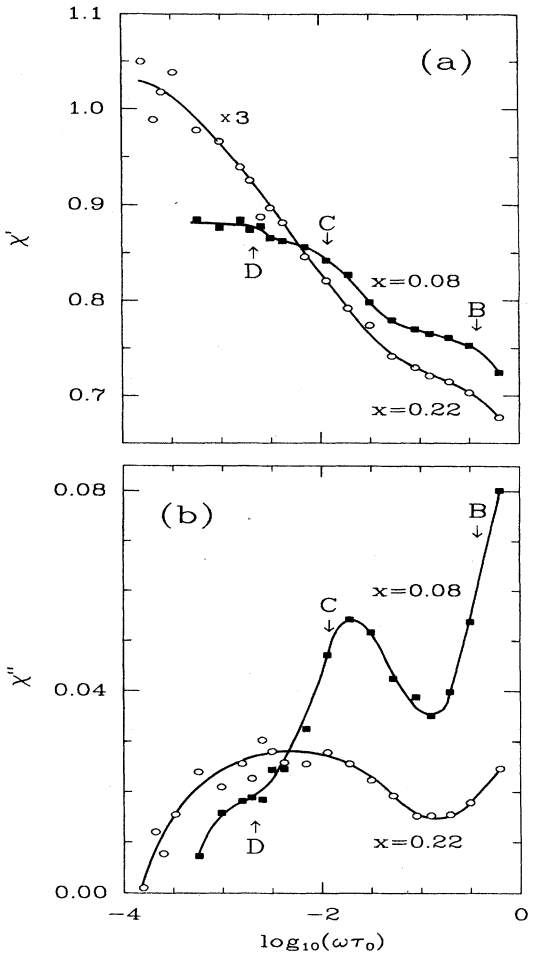

FIG. 6. Frequency dependence of the dynamical susceptibility per spin: (a) the real part and (b) the imaginary part. The susceptibility is in units of $1/|J|$. The solid squares refer to the system below the percolation threshold and the open circles to the system just above it. The capital letters and the arrows identify typical values of relaxation times in regions corresponding to the consecutive values of the discrete barriers. The temperature is equal to $0.5|J|$.

inverses of the typical relaxation times corresponding to the regions B, C, D, and so on. It should be noted that this structure is less pronounced than that shown in Ref. 18 simply because we study the susceptibility at $T=0.5$ and not at 0.2. The structure in the susceptibility reflects the physics of some processes being frozen and other undergoing relaxation in the time domain under study. The identification of the relevant time scales is consistent with the one made when discussing the time dependent correlations. The A region is too short lived to be seen.

The structure in the frequency dependence of the susceptibility is less sharp in the system generated at $x=0.22$, but it is still noticeable. At this temperature we can identify two maxima in χ''. One of these corresponds to the D region (or D mixed with C) and the other to the B region (or, more likely to B overlapping with C). Like in the discussion of the time delayed correlations, region

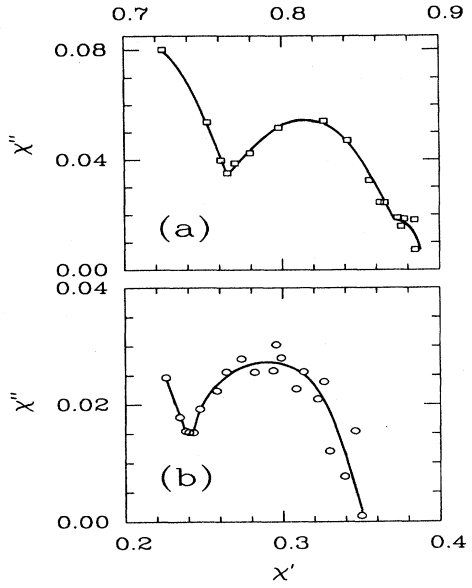

FIG. 7. The Argand plots of χ'' vs χ': (a) is for $x=0.08$ and (b) is for $x=0.22$.

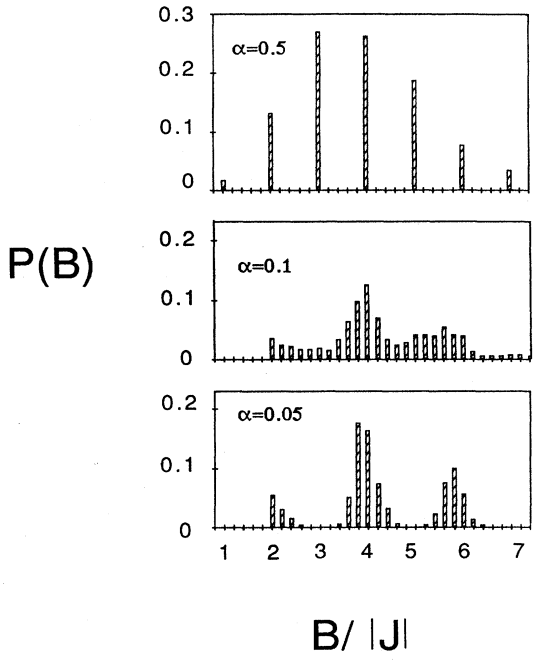

FIG. 8. Distribution of energy barriers for the energy minima generated in systems with the next-neighbor interactions present. The ratio, α, of the antiferromagnetic next-neighbor coupling J_{NN} to the nearest-neighbor coupling J is indicated. Here $L=4$ and $x=0.20$.

C is hard to identify. It is possible that this could be enabled by considering still smaller T (which was beyond our reach). The structure in the susceptibility is also seen on the so called Argand plots shown in Fig. 7. For a continuous spectrum of relaxation times the Argand plots reduce to an ellipse, but Fig. 7 shows sections of several different elliptic curves which are joined together. This indicates gaps in the spectrum. Note also that for $x=0.08$ we do see three elliptic pieces, but regions C and D (the smallest piece) overlap. We conclude that the susceptibility $x>x_c$ exhibits a structure which seems to mirror the discrete structure of barriers.

VI. INFLUENCE OF THE NEXT-NEAREST NEIGHBORS

We now come back to the question of the observability of the predicted structure in the dynamic susceptibility. Within the framework of the Ising model there is at least one mechanism which may smooth the structure out and this is the presence of the next-neighbor couplings. Whether these couplings have such a "destructive" influence on the relaxation spectrum seems to depend on the ratio, α, of these couplings, J_{NN}, to J as shown in Fig. 8. In this figure we show a distribution of the barriers for three values of α. The barriers were calculated for local energy minima generated in the system of $x=0.20$ and $L=4$. If α is equal to 0.5, then the distribution of the barriers still has a discrete nature, but the barriers now come in multiples of $|J|$ and not $2|J|$. Thus one would need much lower temperatures to observe a structure in the susceptibility (if any). On the other hand, if α is very small, then the barriers group in the immediate vicinities of the values which are multiples of $2|J|$ and the gaps in the spectrum should still be present. Finally, for an intermediate value of α of, say, 0.1, the spectrum becomes quasicontinuous with no expectations for the spectrum of relaxation times to contain gaps. This probably dooms $Cd_{1-x}Mn_xTe$ as candidate for a system in which the structure could be observed. Note, however, that it is not clear how to "translate" experimental data on the exchange couplings into the effective ones to be used in an Ising model. Second, it is not clear how next-neighbor couplings affect the very largest barriers due to the lowest states.

In a recent paper, Rigaux *et al.*[31] report on measurements of the dynamical susceptibility of a sister compound $Hg_{1-x}Mn_xTe$ at several values of frequency (between 600 and 3000 Hz and $x=0.35$, $T=9$ and 10 K. It appears that no structure is present[32] but the frequency window is too narrow to set the issue. On the other hand, Geschwind *et al.*[33] consider $Cd_{1-x}Mn_xTe$ in a highly concentrated regime of $x=0.65$. In this regime the system is an antiferromagnet of the third kind. Due to high connectivity at this x, the barriers probably take only high values and the relaxation times should be studied at long time scales. The focus of the paper, however, does not relate to a possible frequency structure in χ. Recently, Klosowski *et al.*[34] have studied another class of fcc compounds: $Zn_{1-x}Co_xS$ and $Zn_{1-x}Co_xSe$ in which $|J|$ is about 96 K. If the next-neighbor couplings are small there, then these might be candidates to look for the frequency structures.

We conclude by suggesting a necessity of further experimental and theoretical studies on this subject. A primary goal of such studies should be the isolation of Heisenberg features from Ising ones in the dynamics of spin glasses.

ACKNOWLEDGMENTS

Discussions with J. R. Banavar, T. Dietl, and T. M. Giebultowicz are greatly appreciated. We acknowledge support from the National Science Foundation through Grants No. DMR-8607150 (M.Z.C.) and DMR-8553271 (M.C.). One of the authors (T.R.G.) has been supported by grants from the Swedish Natural Science Research Council and he appreciates hospitality of the University of Lund.

---

*On leave from Institute of Physics, Polish Academy of Sciences, 02-668 Warsaw, Poland.

†On leave of absence from Institute of Theoretical Physics, Warsaw University, 00-681 Warsaw, Poland.

[1]P. W. Anderson, Phys. Rev. **79**, 705 (1950); J. M. Luttinger, *ibid.* **81**, 1015 (1951).

[2]A. Danielian, Phys. Rev. Lett. **6**, 670 (1961); Phys. Rev. **133**, A1344 (1964).

[3]K. Binder, Phys. Rev. Lett. **45**, 811 (1980); O. J. Heilmann, J. Phys. A **13**, 1803 (1980).

[4]C. L. Henley, J. Appl. Phys. **61**, 3962 (1987).

[5]See also T. M. Giebultowicz, J. Magn. Magn. Mater. **54–57**, 1287 (1986).

[6]W. Y. Ching and D. L. Huber, J. Appl. Phys. **52**, 1715 (1981).

[7]G. S. Grest and E. G. Gabl, Phys. Rev. Lett. **43**, 1182 (1979); J. F. Fernandez, H. A. Farach, C. P. Poole, and Puma, Phys. Rev. B **27**, 4274 (1983); H. A. Farach, R. J. Creswick, J. M. Knight, C. P. Poole, and J. F. Fernandez, *ibid.* **31**, 3188 (1985).

[8]J. R. Banavar and M. Cieplak, Phys. Rev. Lett. **48**, 832 (1982); B. W. Morris, S. G. Colborne, M. A. Moore, A. J. Bray, and J. Canisius, J. Phys. C **19**, 1157 (1986); A. Chakrabarti and C. Dasgupta, Phys. Rev. Lett. **56**, 1404 (1986).

[9]K. Binder and A. P. Young, Rev. Mod. Phys. **58**, 801 (1986); A. J. Bray and M. A. Moore, in *Heidelberg Colloquium on Glassy Dynamics*, edited by L. Van Hemmen and I. Morgenstern (Springer, Berlin 1987), p. 121.

[10]R. R. Galazka, S. Nagata, and P. H. Keesom, Phys. Rev. B **22**, 3344 (1980); T. Giebultowicz, H. Kepa, B. Buras, K. Clausen, and R. R. Galazka, Solid State Commun. **40**, 499 (1980); R. R. Galazka, J. Cryst. Growth **72**, 364 (1985); J. K. Furdyna, J. Appl. Phys. **53**, 7637 (1982); T. Dietl, Jpn. J. Appl. Phys. **26**, Suppl. 26–3, 1907 (1987).

[11]J. J. Hauser and J. V. Waszczak, Phys. Rev. B **30**, 5167 (1984).

[12]N. Samarth and J. K. Furdyna, Phys. Rev. B **37**, 9227 (1988); see also B. E. Larson and H. Ehrenreich, Phys. Rev. B **39**, 1747 (1989).

[13]A. Chakrabarti and C. Dasgupta, Phys. Rev. B **36**, 793 (1987).

[14]J. Spalek, A. Lewicki, Z. Tarnawski, J. K. Furdyna, R. R. Galazka, and Z. Obuszko, Phys. Rev. B **33**, 3407 (1986).

[15]T. M. Giebultowicz, J. J. Rhyne, W. Y. Ching, and D. L. Huber, J. Appl. Phys. **57**, 3415 (1985); W. Y. Ching, D. L. Huber, J. K. Furdyna, B. Lebech, and R. R. Galazka (unpublished).

[16]M. Escorne and A. Mauger, Phys. Rev. B **25**, 4674 (1982); A. Lewicki, J. Spalek, J. K. Furdyna, and R. R. Galazka, *ibid.* **37**, 1860 (1988).

[17]For a discussion of spin waves on a fully and partially occupied fcc lattice of Heisenberg spins see, e.g., W. Y. Ching and D. L. Huber, Phys. Rev. B **25**, 5761 (1982); **26**, 6164 (1982).

[18]M. Cieplak, M. Z. Cieplak, and J. Lusakowski, Phys. Rev. B **36**, 620 (1987).

[19]M. Cieplak and G. Ismail (unpublished).

[20]K. Gunnarsson, P. Svedlindh, P. Nordblad, L. Lundgren, H. Aruga, and A. Ito, Phys. Rev. Lett. **61**, 754 (1988).

[21]J. R. Banavar, M. Cieplak, and M. Muthukumar, J. Phys. C **18**, L157 (1985); M. Cieplak and J. Lusakowski, *ibid.* **19**, 5253 (1986).

[22]W. L. McMillan, Phys. Rev. B **28**, 5216 (1983).

[23]W. L. McMillan, Phys. Rev. B **30**, 476 (1984).

[24]J. R. Banavar and M. Cieplak (unpublished).

[25]R. Rammal and Benoit, J. Phys. Lett. **46**, L-667 (1985).

[26]J. Banavar, M. Cieplak, and T. R. Gawron (unpublished).

[27]R. Glauber, J. Math. Phys. **4**, 294 (1963).

[28]In Ref. 18 we used a notation: $\tau_0' = a\tau_0$.

[29]D. S. Fisher and D. A. Huse, Phys. Rev. B **38**, 373 (1988); **38** 386 (1988), and references therein.

[30]M. Cieplak and G. Szamel, Phys. Rev. B **37**, 1790 (1988).

[31]C. Rigaux, A. Mycielski, G. Barilero, and M. Menaut, Phys. Rev. B **34**, 3313 (1986).

[32]A. Mycielski, private communication.

[33]S. Geschwind, A. T. Ogielski, G. Devlin, J. Hegarty, and P. Bridenbaugh, J. Appl. Phys. **63**, 3291 (1988).

[34]P. Klosowski, T. M. Giebultowicz, and J. K. Furdyna, private communication.